# Studies on Aerosol-Cloud Interaction and Weather Modification using MRI Cloud Simulation Chamber

Masataka MURAKAMI[1,2], Takuya TAJIRI[2] and Narihiro ORIKASA[2]

1 Institute for Space-Earth Environmental Research, Nagoya University
2 Meteorological Research Institute, Japan Meteorological Agency

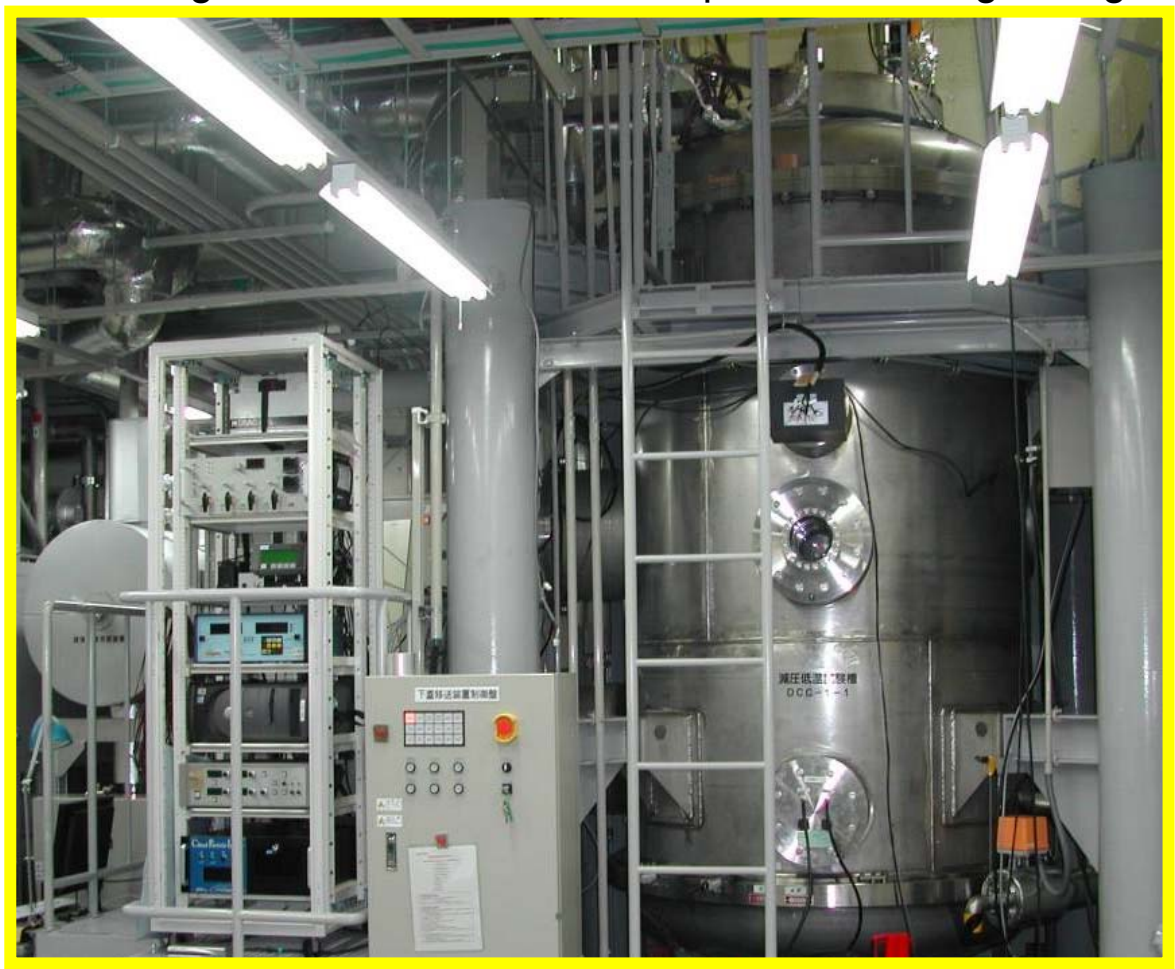

Workshop on Laboratory Facilities for Cloud Research, Sep. 24, 202

# MRI Cloud Simulation Chamber

- To investigate the details of the fundamental processes of cloud formation, MRI cloud simulation chamber was built in 2004.
- MRI cloud chamber design was based on the adiabatic-expansion-type chamber of CSU, wherein the wall temperature and air pressure are simultaneously controlled in the experimental volume to simulate natural cloud formation processes (adiabatic expansion).
- MRI cloud chamber improves on CSU's in terms of the range of experimental conditions (temperature, pressure and evacuation/cooling rates), the accuracy of the simultaneous control of wall temperature and air pressure, and the number, quality, and capabilities of particle measuring instrumentation for documenting evolution of aerosol and cloud particle concentrations, size, and phase.

Cold Environment Simulator Building

External Appearance

Control Panel

## Air Conditioning & Measurement

View Laser (left)
Fan Agitator

Pressure
Transducer

Chilled Mirror
Hygrometers

Experimental Working Volume

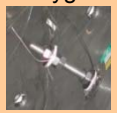

Thermocouples
Attached to The
Chamber Wall

## Cooling and Evacuation Air System

Anti-freeze Fluid
Circulation-pump

Refrigerators

Liquid Nitrogen Cylinder

Vacuum Pump

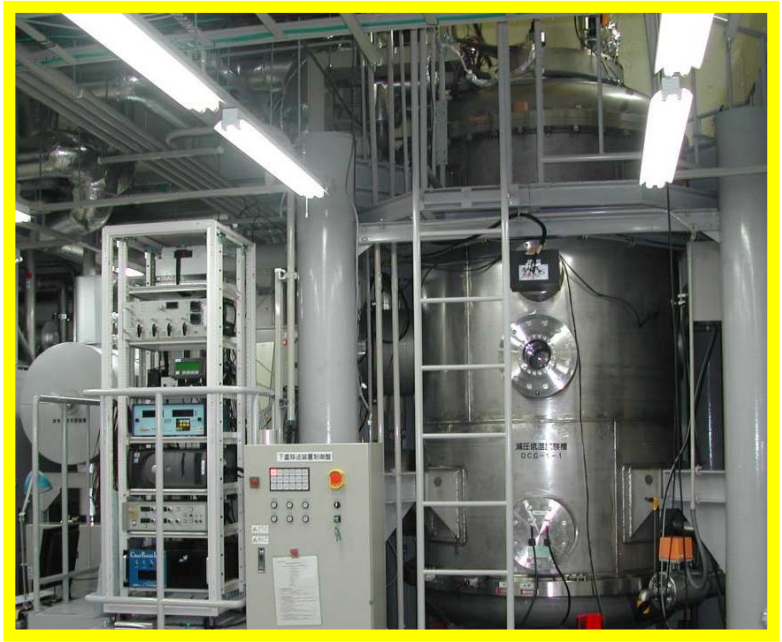

## Devices for Particle Detection

## Laser Sensor

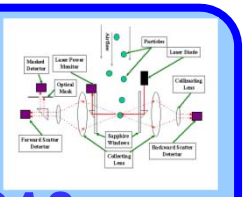

## CAS

## View Port

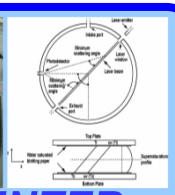

## Wyoming CCN COUNTER

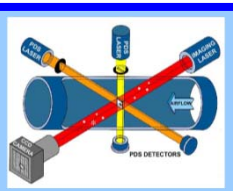


## CPI

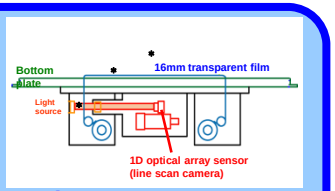


## Microscopic Ice Crystal Detector

# MRI CLOUD SIMULATION CHAMBER FACILITY

# Basic features of MRI camber

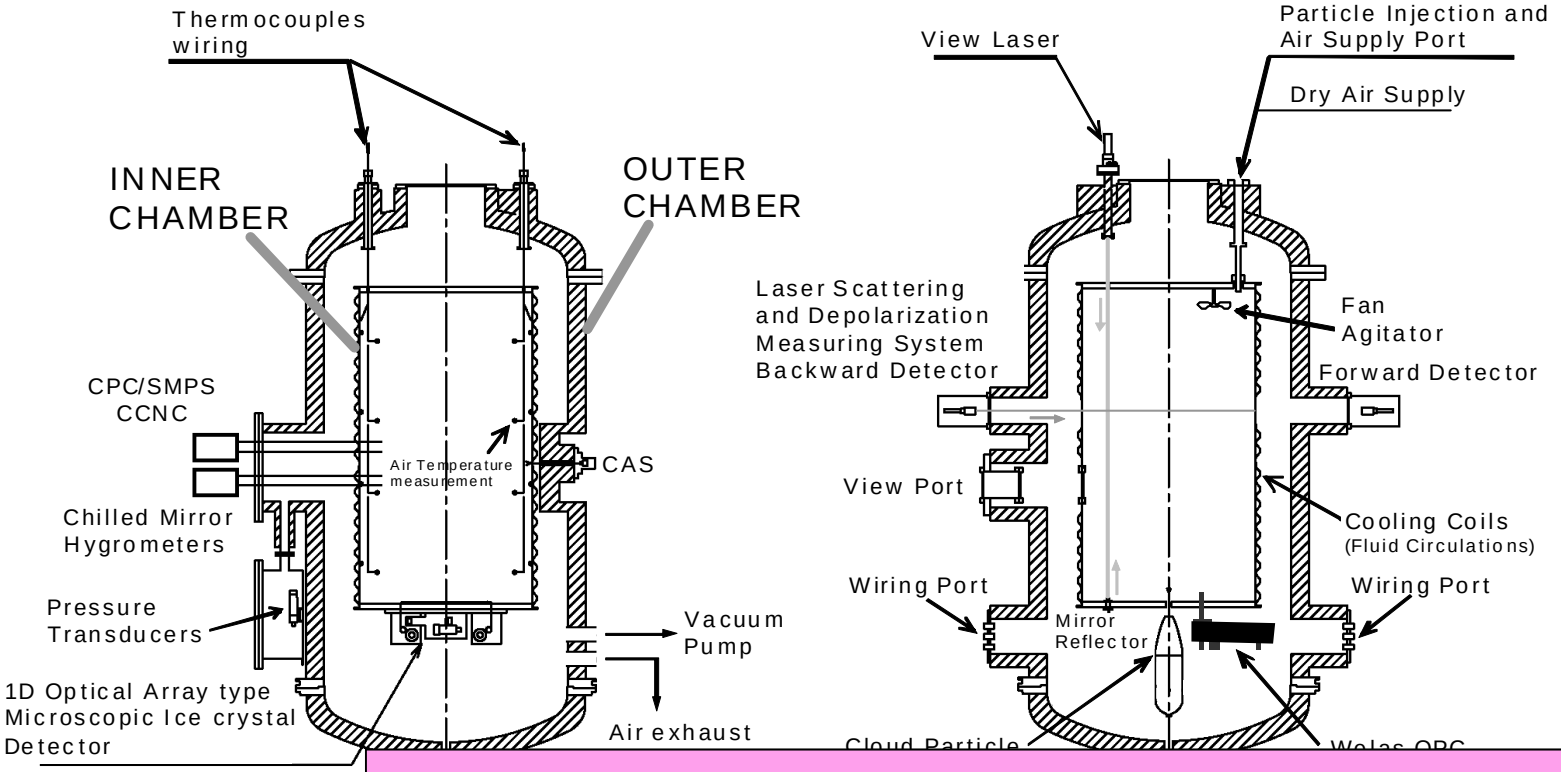


Air is evacuated from the outer vessel
Evacuation creates an adiabatic cooling of the air
Tw is controlled to match Ta
Inner vessel can be cooled by circulating anti-freeze fluid
Fluid paths are subdivided into seventeen panels
Air temperature inhomogeneity is
within ±0.3 C under no expansion conditions
within ±1.5 C during an expansion (W = 10 m $s^{-1}$)

**Operational Ranges**

**Pressure inside Chamber**

**Wall Temperature**

**Estimated Ascent Rate**

# MRI Cloud Simulation Chamber

## (Particle Measuring System)

Cloud Particles

Adiabatic expansion process
(Cloud formation)

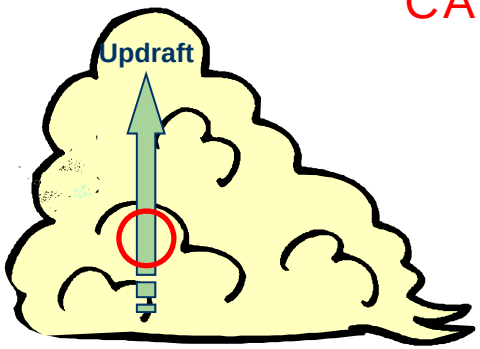


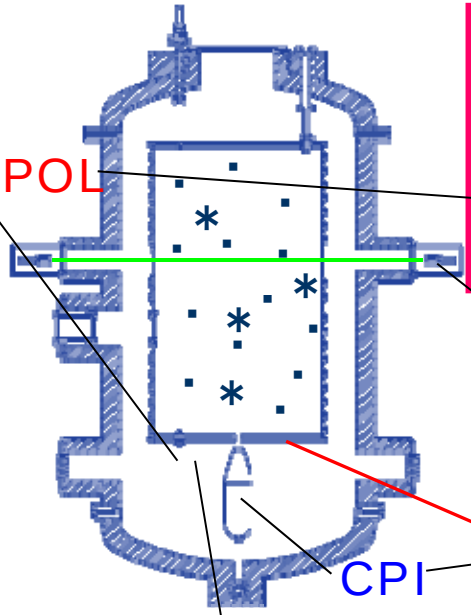


Laser sensor

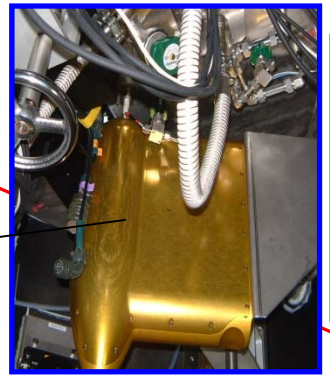

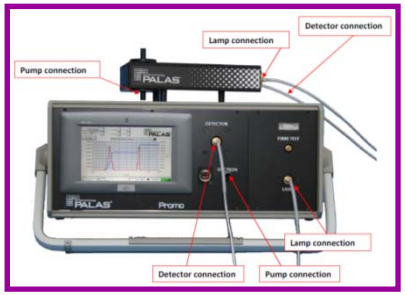


Welas OPC

Aerosol Particles

CCN Counter
(CCN-200, DMT)

IN Counter
(MRI)

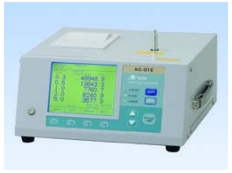

OPC
(KC-01E, RION)

SMPS
(MODEL3936, TSI)

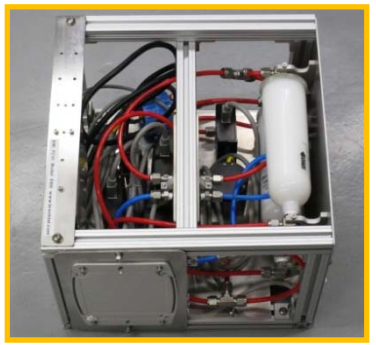

Tajiri et al. 2013

# Preconditioning Method

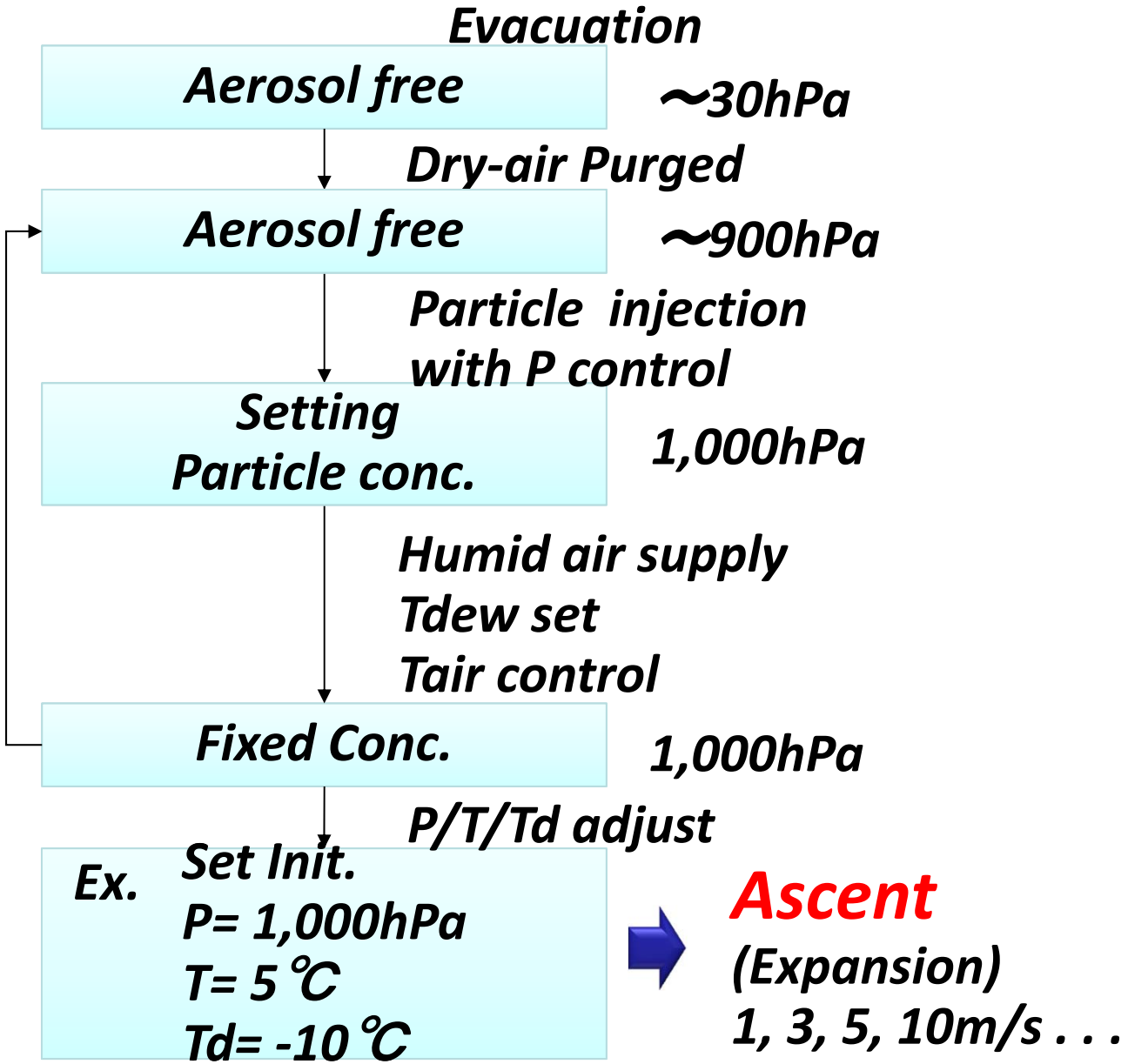

# Aerosol Measurement Building

Internally mixed aerosol generator

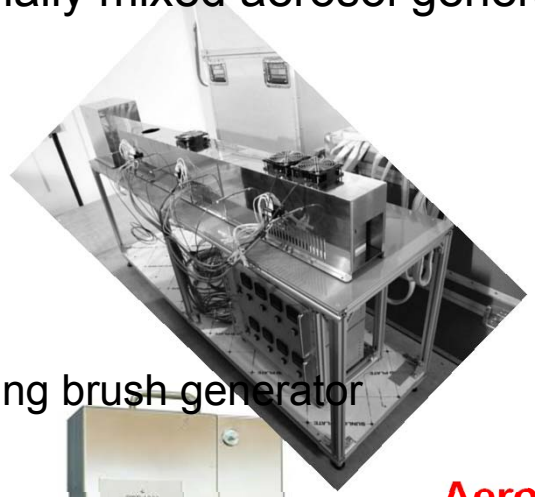

Aerosol inlets on the roof

Rotating brush generator

Aerosol Buffer tank

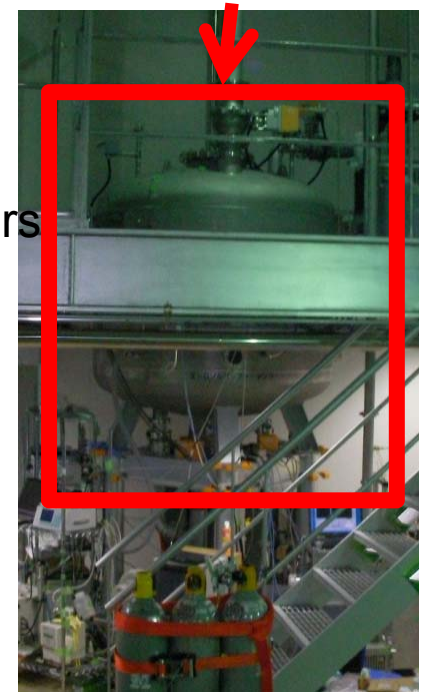

SMPS OPC CCNC INC

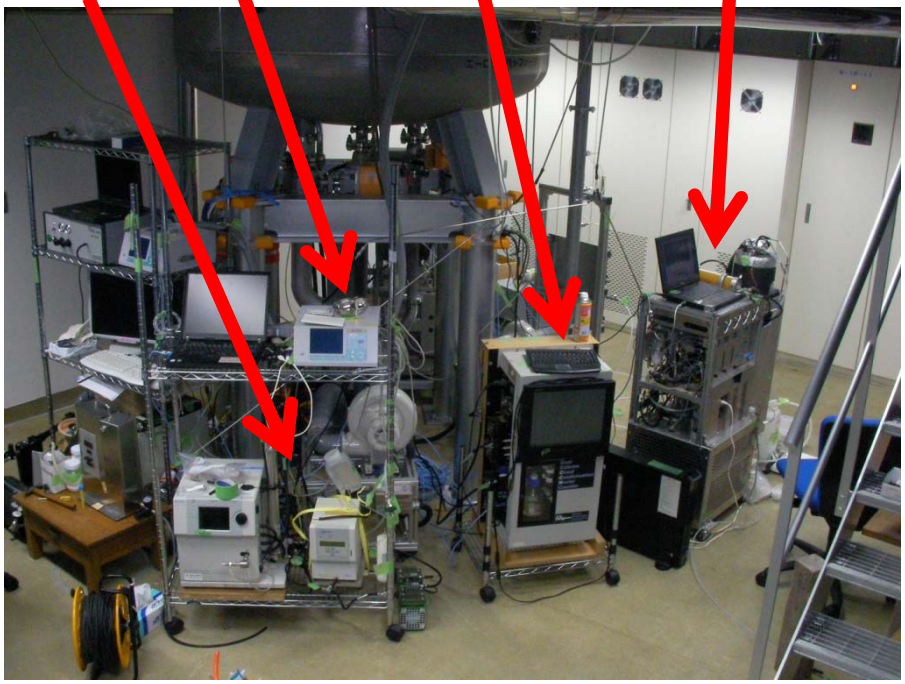

graphite spark generators


Atomizer aerosol generator

# Advantage of MRI Cloud Chamber

## (an adiabatic-expansion-type cloud chamber)

- Temporal evolution of thermodynamic properties experienced by air and aerosol particles going into clouds are reproduced as closely as possible to rising air parcels in the atmosphere.
- Wide range of air temperature to even above 0 C, can be reproduced.
- Wide range of updraft velocities, or equivalently, cooling rates of air, moistening rates of air below cloud bases and production rates of supersaturation above cloud bases can be reproduced.
- Cloudy conditions can be maintained for longer time periods compared with the AIDA chamber.

Such thermodynamic histories, both before and after cloud formation, are important to evaluate the ability of aerosol particles to act as CCN and IN, and to understand their effects on the initial microphysical structures of clouds.

# Limitation of MRI Cloud Chamber

- Cloud lifetime and maintenance of adiabatic condensate amounts is constrained by the gradual sedimentation of large cloud particles and water vapor deposition onto wall with sub-freezing temperatures.

# Setup parameters for two preliminary experiments

| | Experiment No. | |
|---|---|---|
| | #1 | #2 |
| Programmed Initial Pressure (hPa) | 1000.0 | 1000.0 |
| Programmed Initial Temperture (℃) | 20.0 | 15.0 |
| Programmed Adiabatic Ascent Rate (m/s) | 3.0 | 3.0 |
| Actual Initial Pressure (hPa) | 1000.0 | 999.9 |
| Actual Initial Air Temperture (℃) | 19.7 | 14.6 |
| Initial Dewpoint Temperature (℃) | 15.4 | -7.5 |
| Pressure at LCL (hPa) | 919 | 696 |
| Temperture at LCL (℃) | 13.1 | -12.7 |
| Ascent Duration at LCL (sec) | 240 | 970 |
| Sample Aerosol | Ammonium Sulfate | Arizona Test Dust |

# Size distributions of ammonium sulfate particles

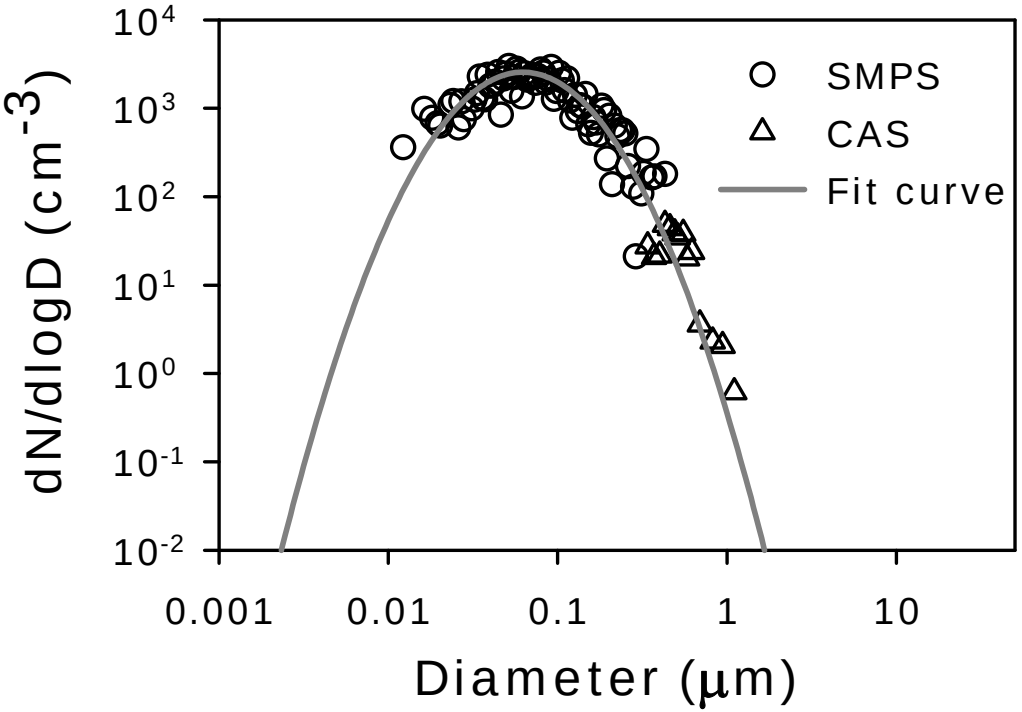


a modal diameter at around 0.08 μm
total concentration about 2,000 $cm^{-3}$

# CCN activation spectrum of ammonium sulfate particles

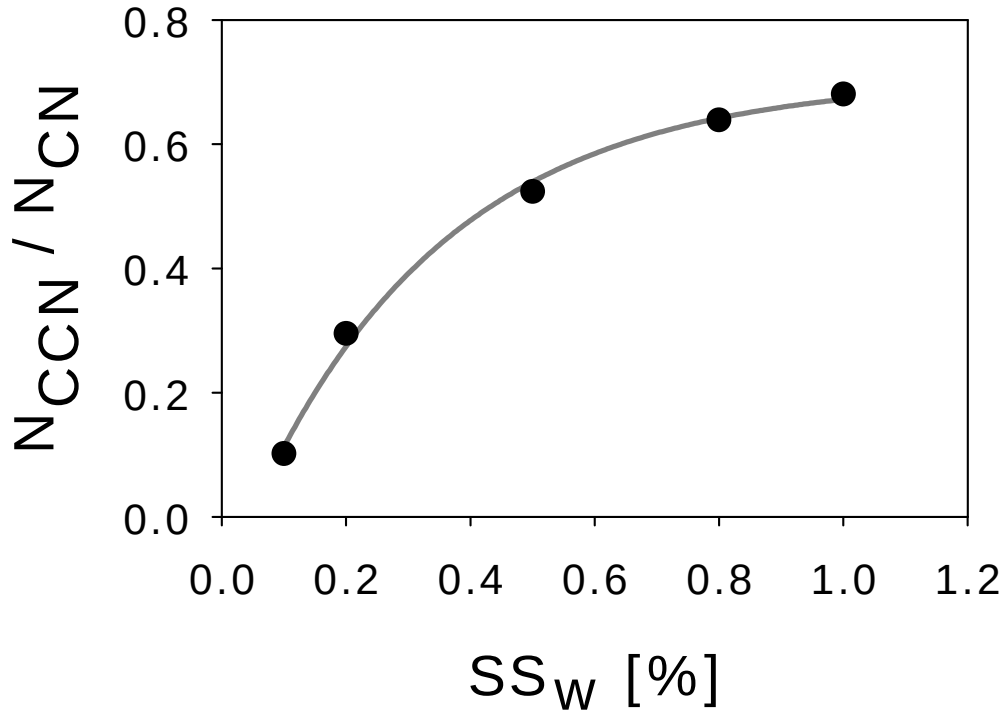


CCN concentrations increased with increasing SSw
about 70 % of ammonium sulfate particles activated as CCN at SSw=1 %

# Warm cloud CCN activation experiment

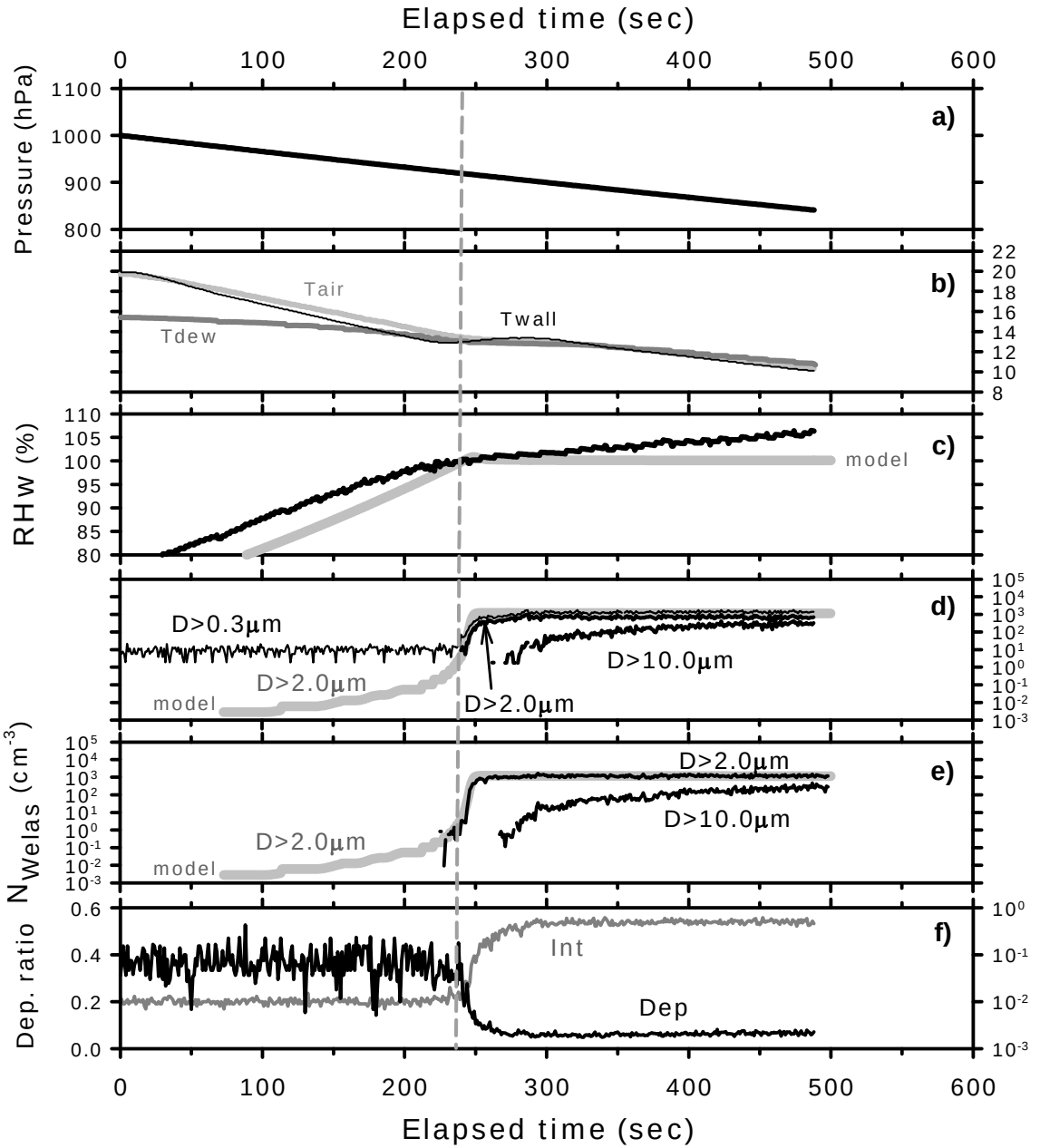


dry adiabatic to moist adiabatic

RHw continued to slightly increase beyond 100%

CDNC attains a peak value of 1,000 $cm^{-3}$, which corresponds approximately to the CCN concentration at SSw = 0.5%.

Detailed bin microphysics parcel model showed a good agreement in CDNC.

# Size distributions of aerosol particles and cloud droplets

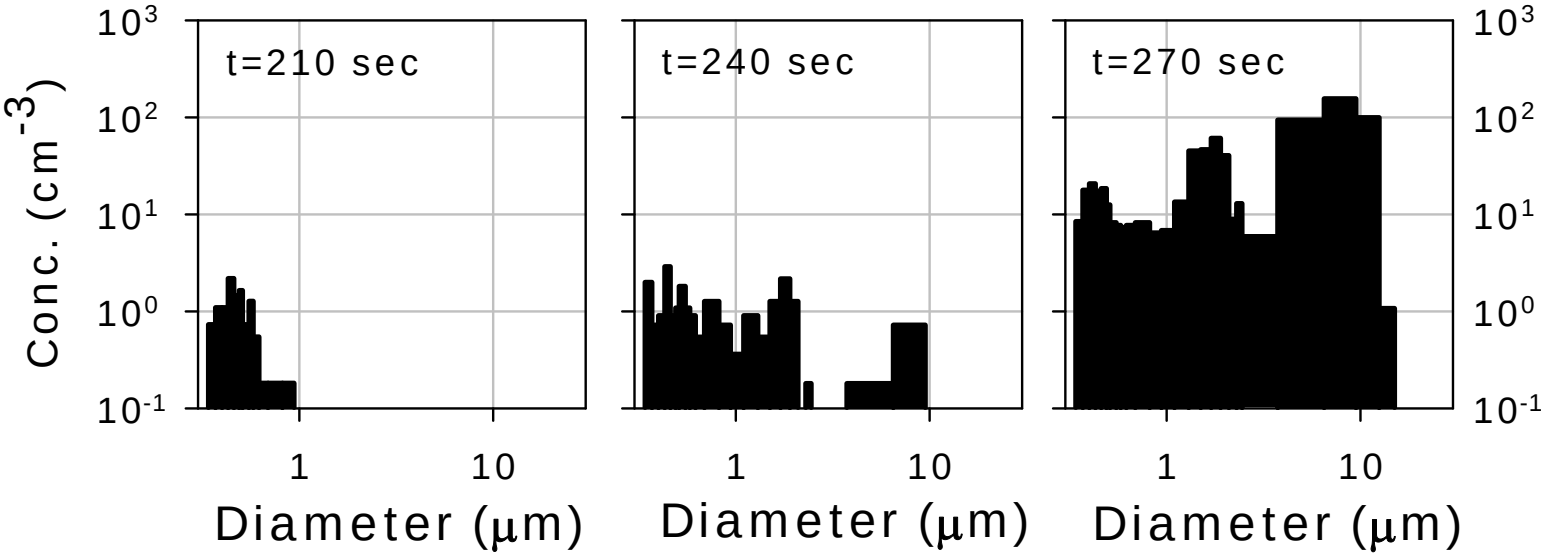


At 210 seconds of elapsed time (30 seconds before the onset of cloud formation), no aerosol particles activated yet.
At 240 seconds, larger aerosol particles started to activate.
Thirty seconds later (t=270 sec), some cloud droplets have grown to 10 μm although the number concentration of cloud droplets is still increasing.

# Size distributions of ATD particles

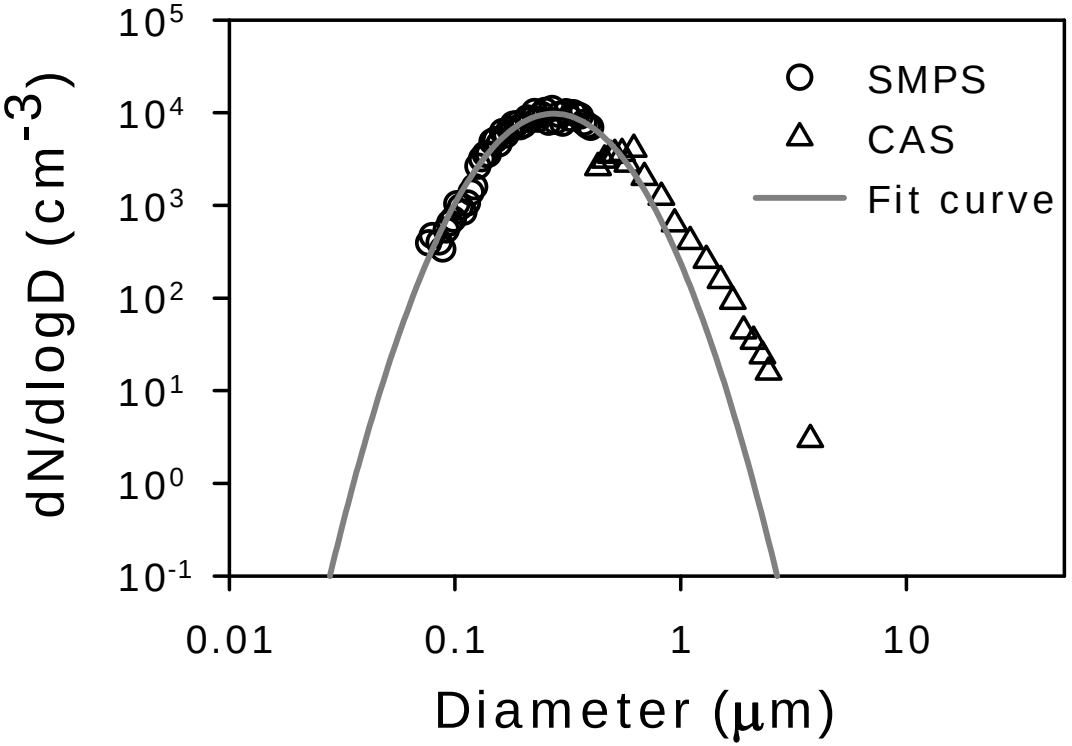


a peak at around 0.5 μm
total number concentrations about 1,000 $cm^{-3}$

# CCN activation spectrum of ATD particles

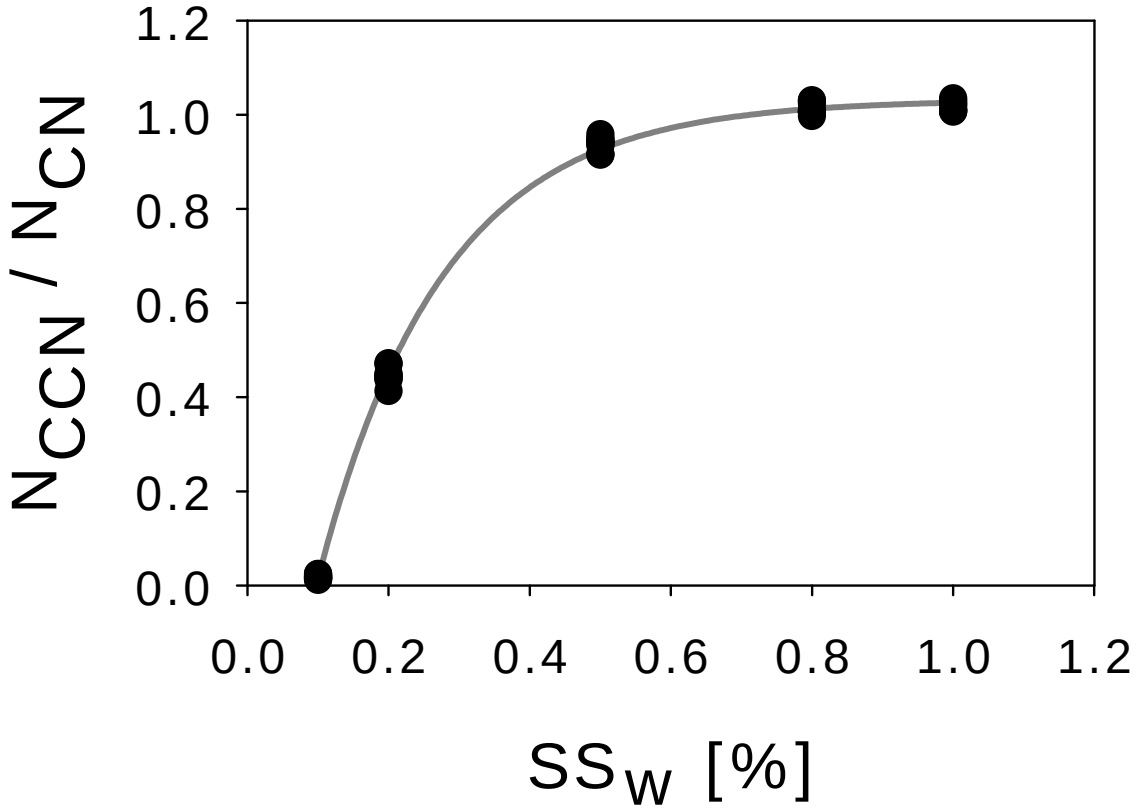


Activated fraction of ATD as CCN were 0.2 at SSw=0.1%, 0.5 at SSw= 0.2% and 1.0 at SSw= 0.8%.

ATD particles by themselves may effectively act as CCN if there are no hygroscopic particles that act as CCN more efficiently than ATD particles.

ATD particles appear to be better CCN than ammonium sulfate, but this is due to their larger sizes.

# Cold cloud IN activation experiment

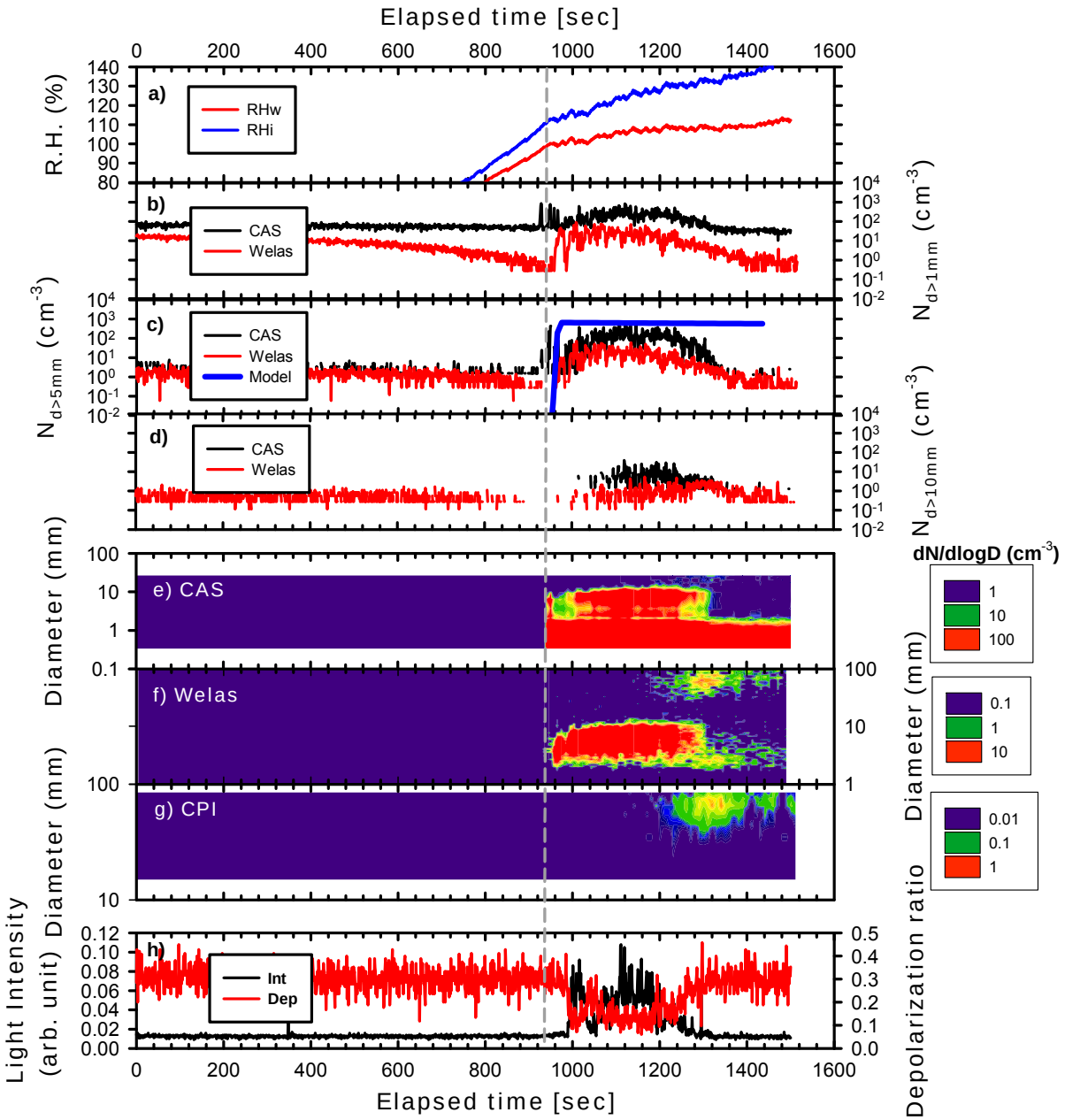


CDNC attains a peak value of 500 $cm^{-3}$, which corresponds to CCN concentration at around SSw = 0.2%.

The max. CDNC was almost consistent with the model prediction .

Onset of ice formation was around -17 C with coexisting supercooled cloud droplets.

The immersion freezing is thought to be the dominant ice nucleation mechanism although the possibility of deposition nucleation cannot be ruled out.

# Activated fractions of ATD as CCN and IN

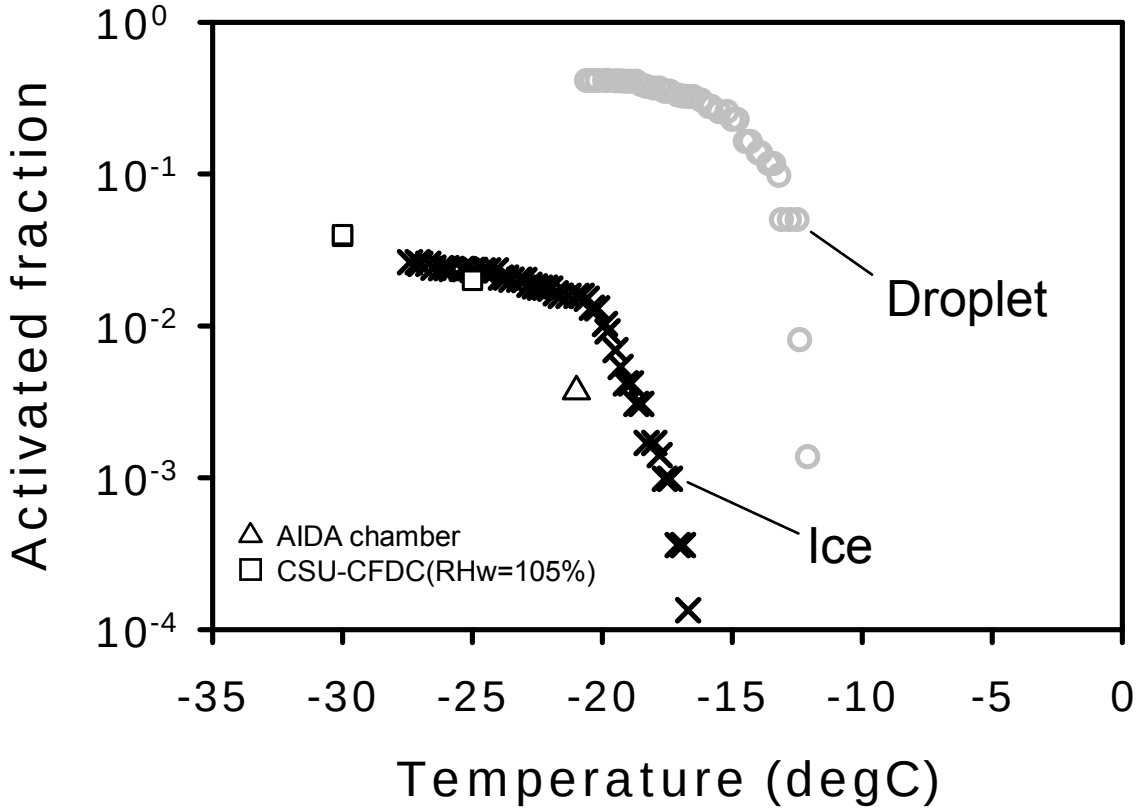


With correction for particle loss due to gravitational sedimentation of ice crystals, cccumulated activated fraction showed a rapid increase at around -17 C due to the immersion freezing and a slight increase below -23 C due to deposition nucleation.

# Images of ice crystals measured with CPI

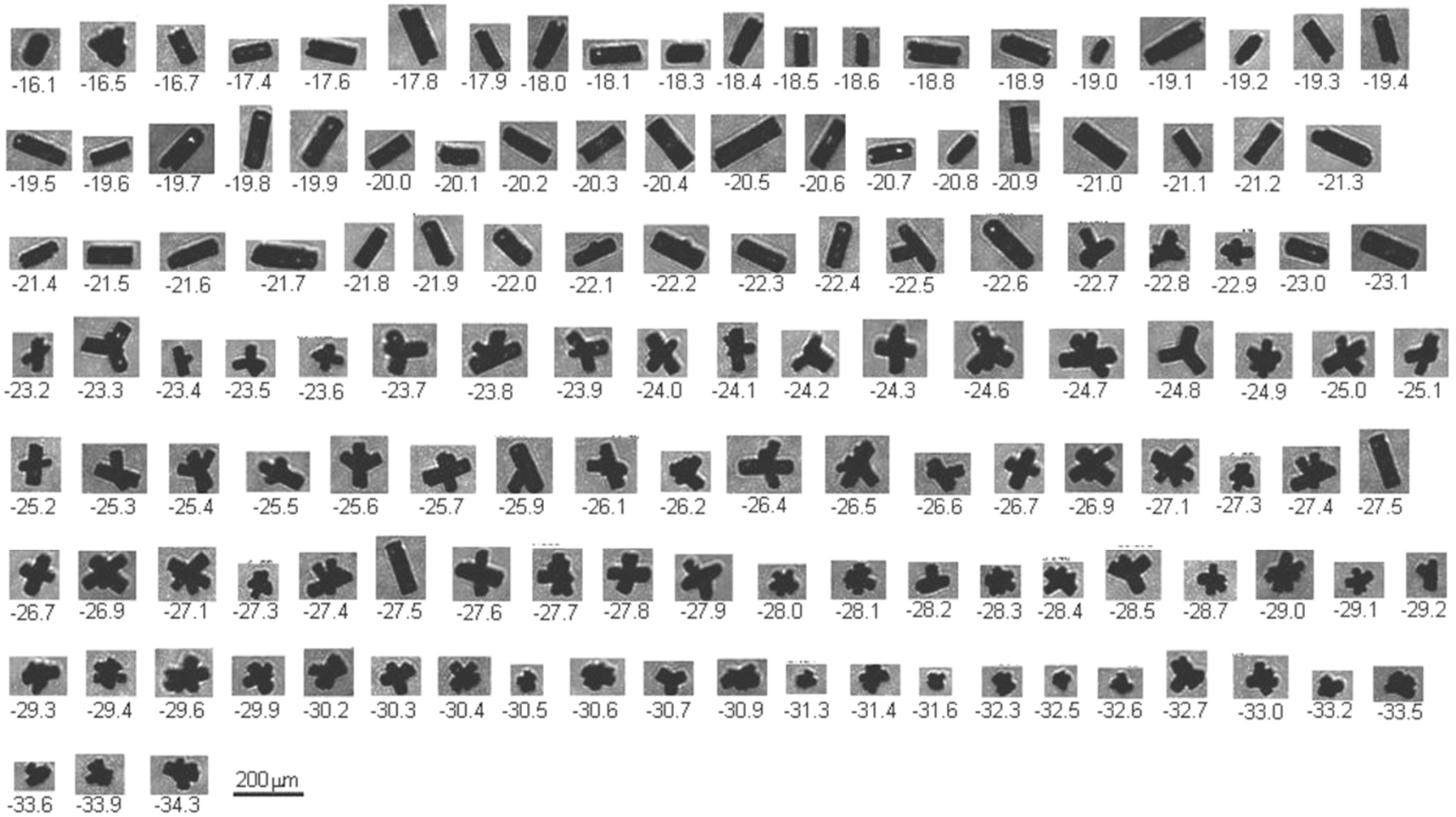


At temperatures lower than -25 C, polycrystalline ice crystals, such as bullet rosettes or combinations of plates and columns, were predominant.

# Characterization of AgI Particles（G-B AgI generator）

Testing Facility for AgI acetone burner

Aerosol, CCN and IN Instruments

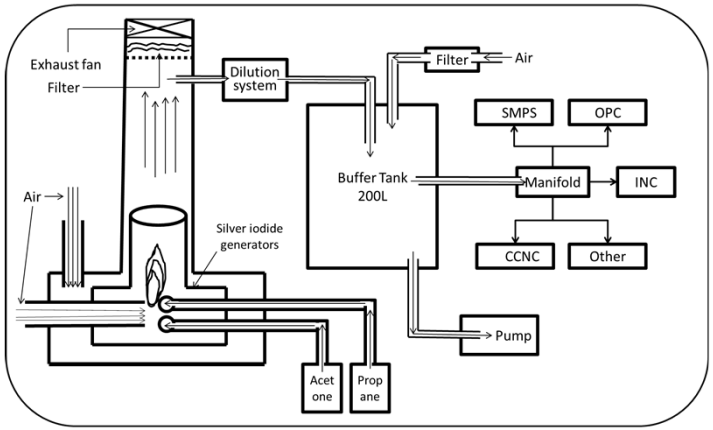


MRI-Dynamic Cloud Chamber

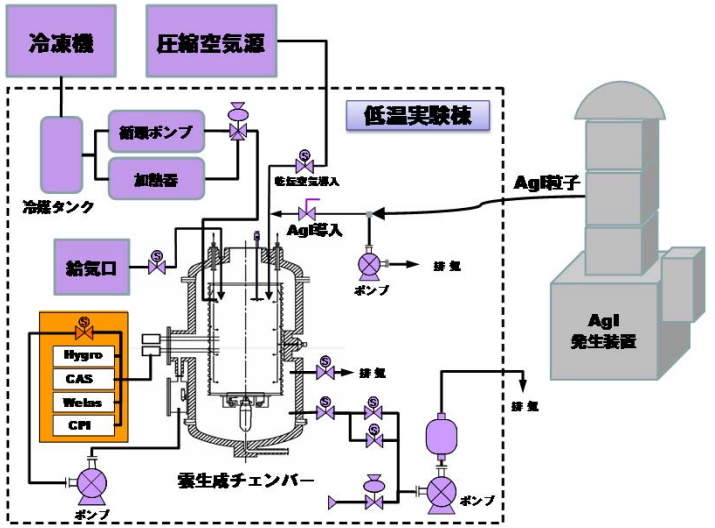

# Size Distribution and Hygroscopicity of AgI Particles

DRI type AgI particles

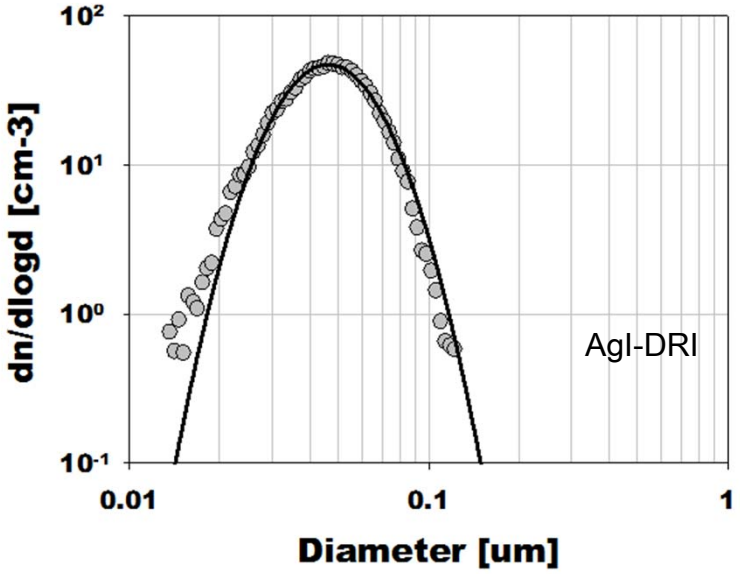


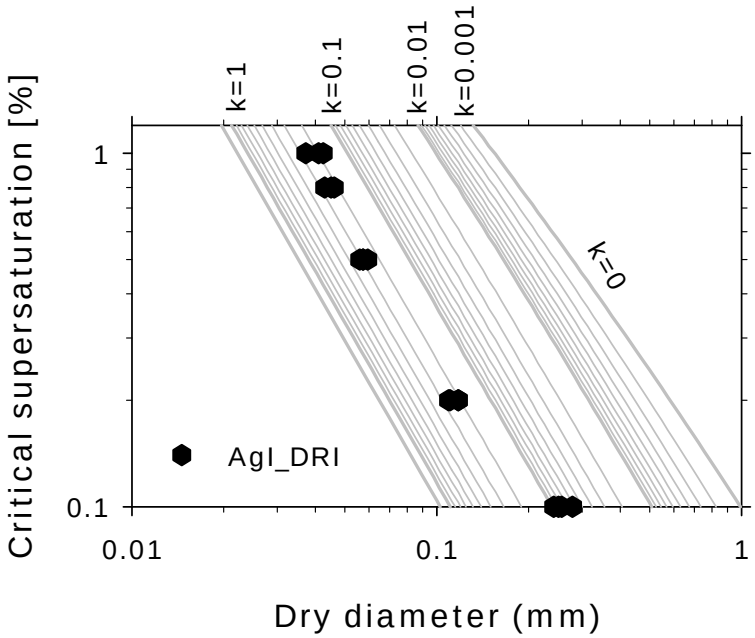

# IN Ability of AgI particles (Comparison)

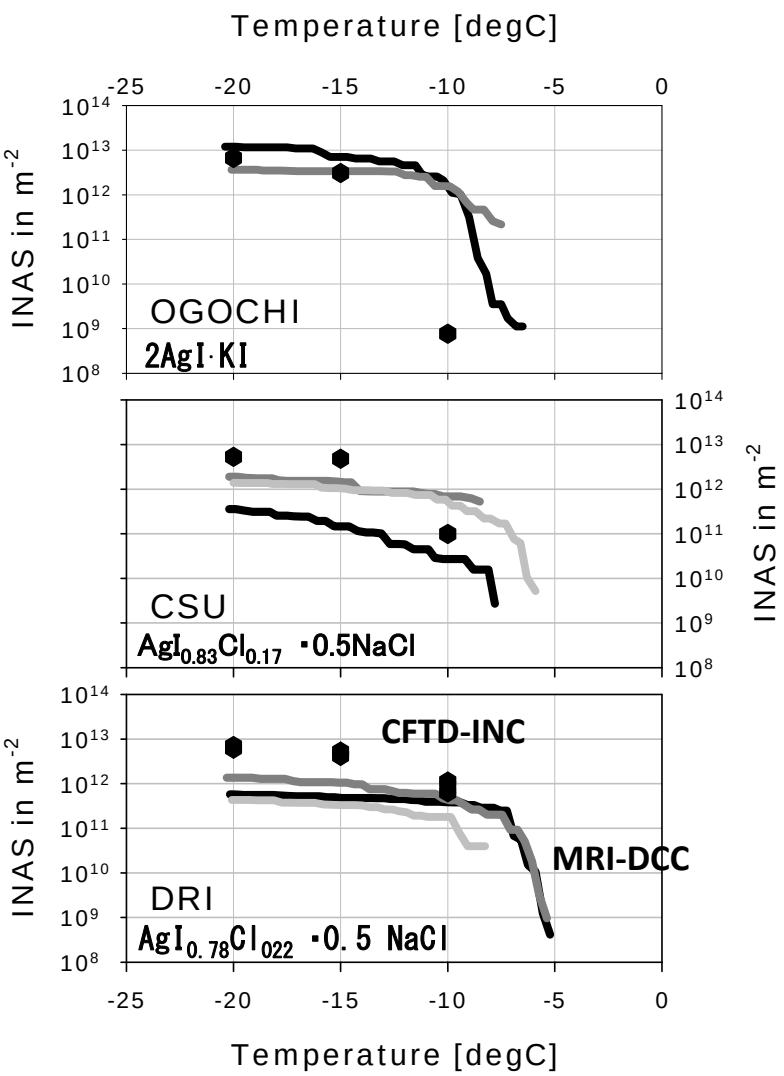


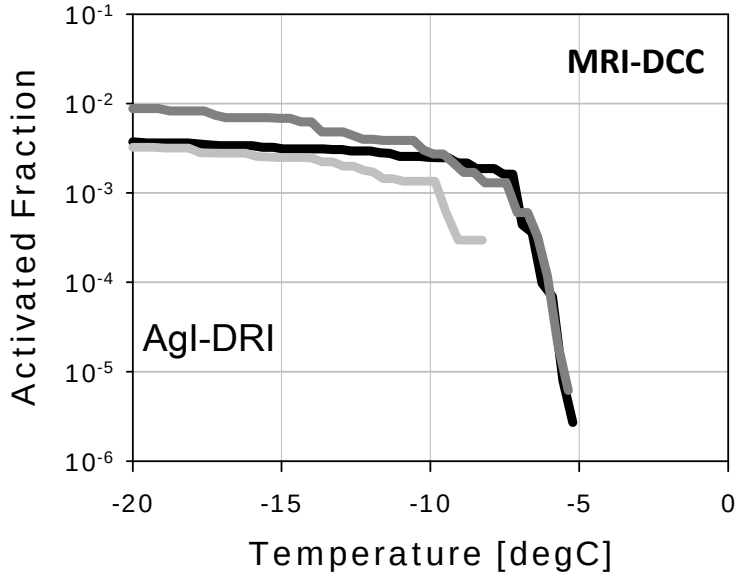


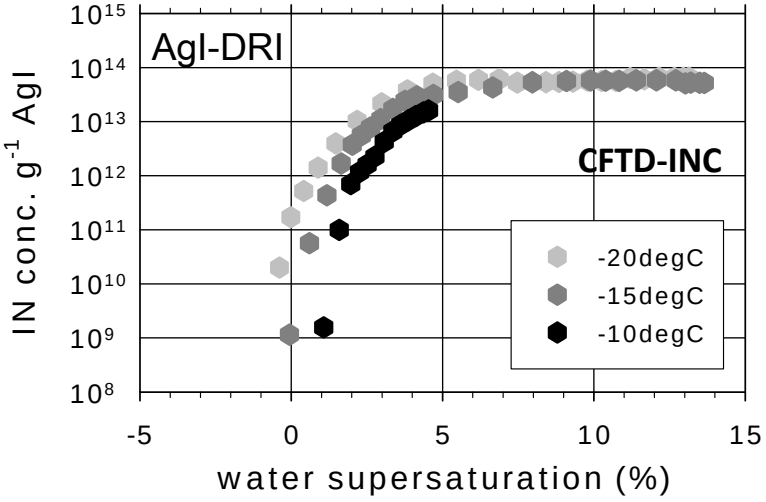

# Chamber Experiment on Hygroscopic Seeding

## Flare Seeding

Flare Test System

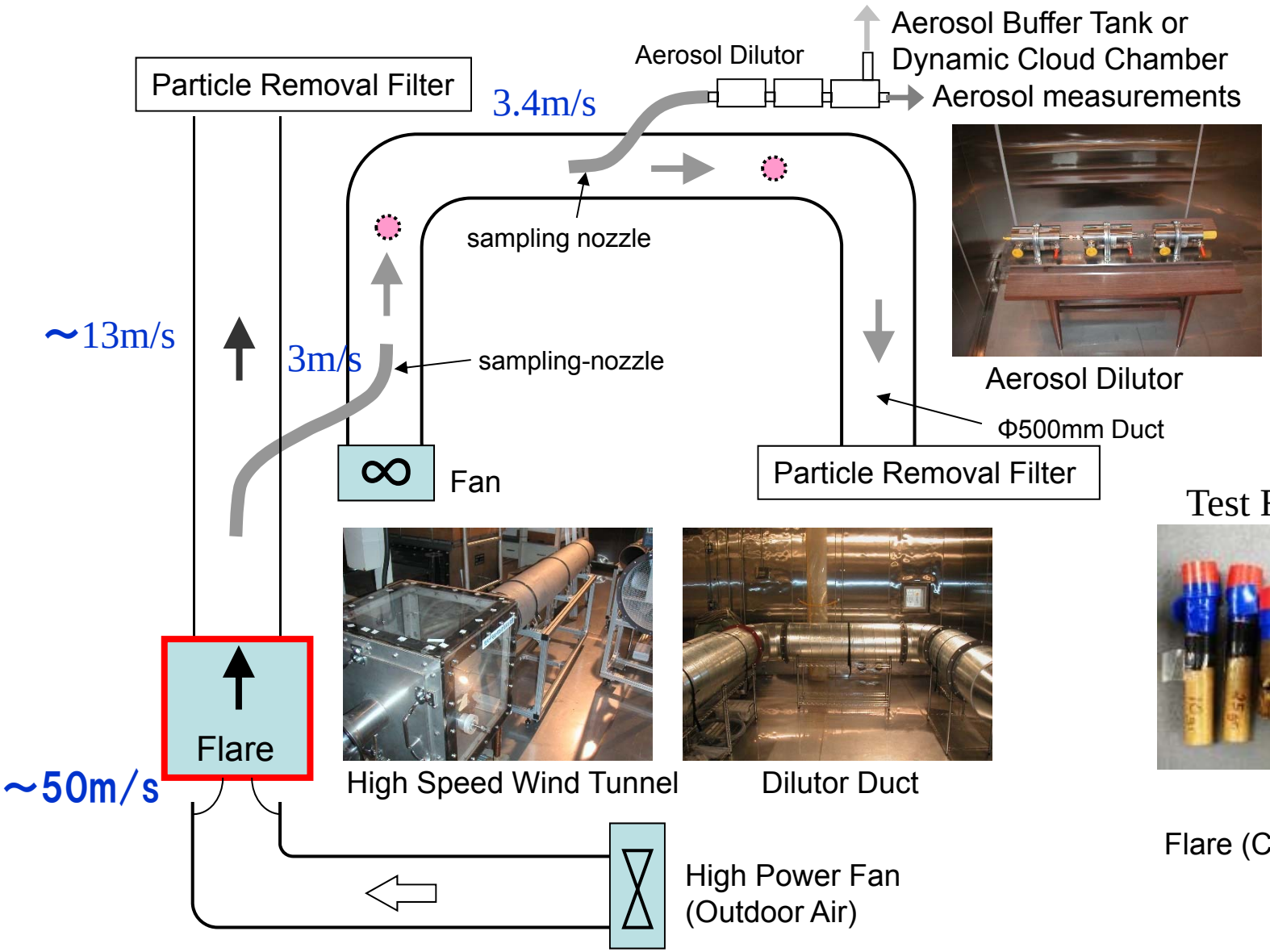




Aerosol Dilutor

Test Flares



Flare (CaCl2, ICE)

# Chamber Experiment on Hygroscopic Seeding

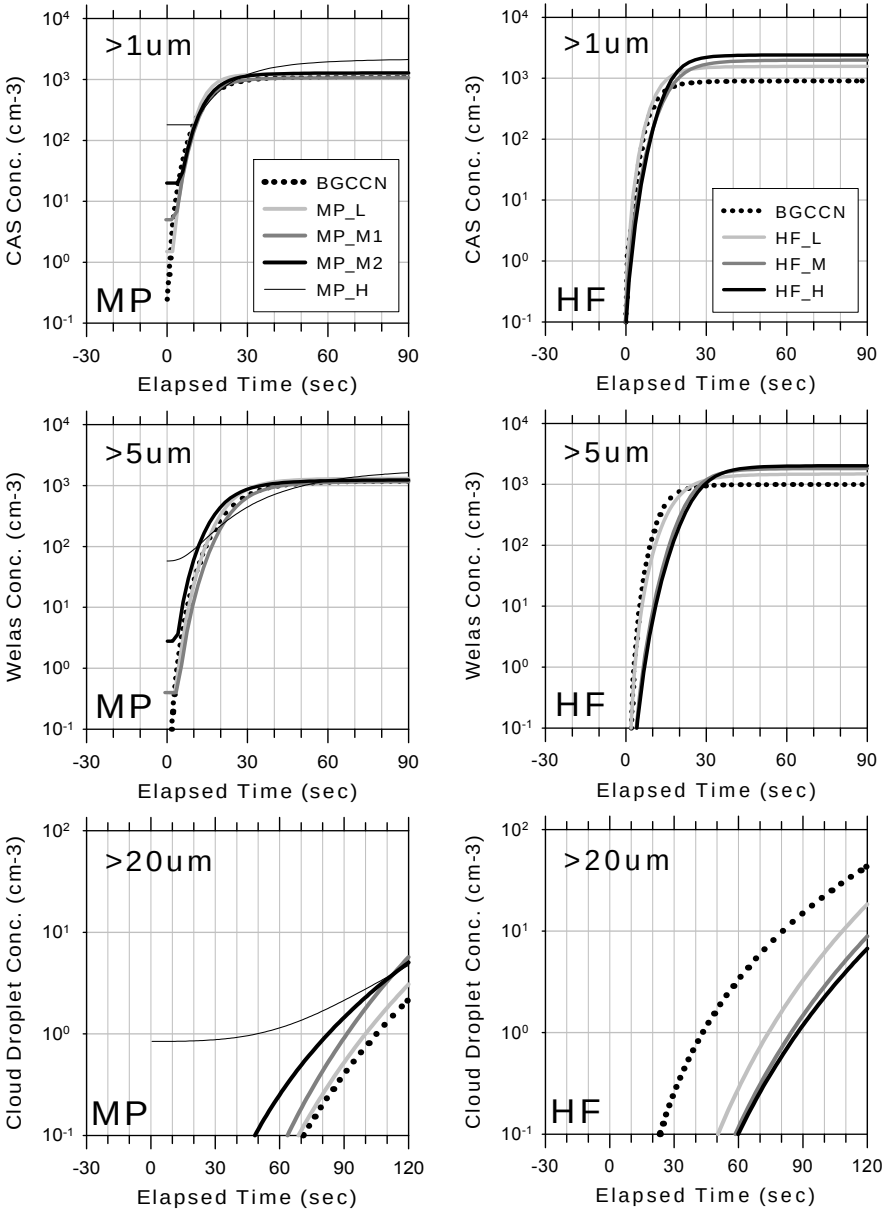


Initial Aerosol Size Distributions

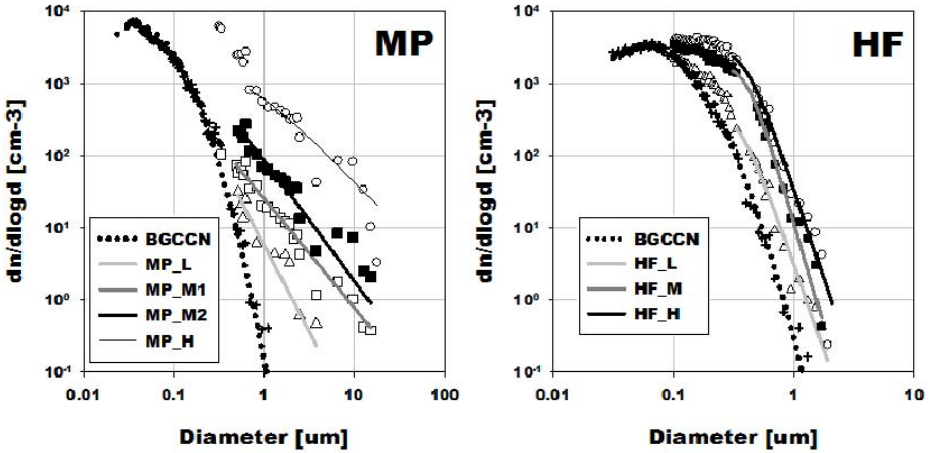


MP
Number of large droplets increases and total number of droplets slightly decreases with increasing the total mass of seeding materials.

Flare
Total droplet conc. increase and number of large droplets decrease.

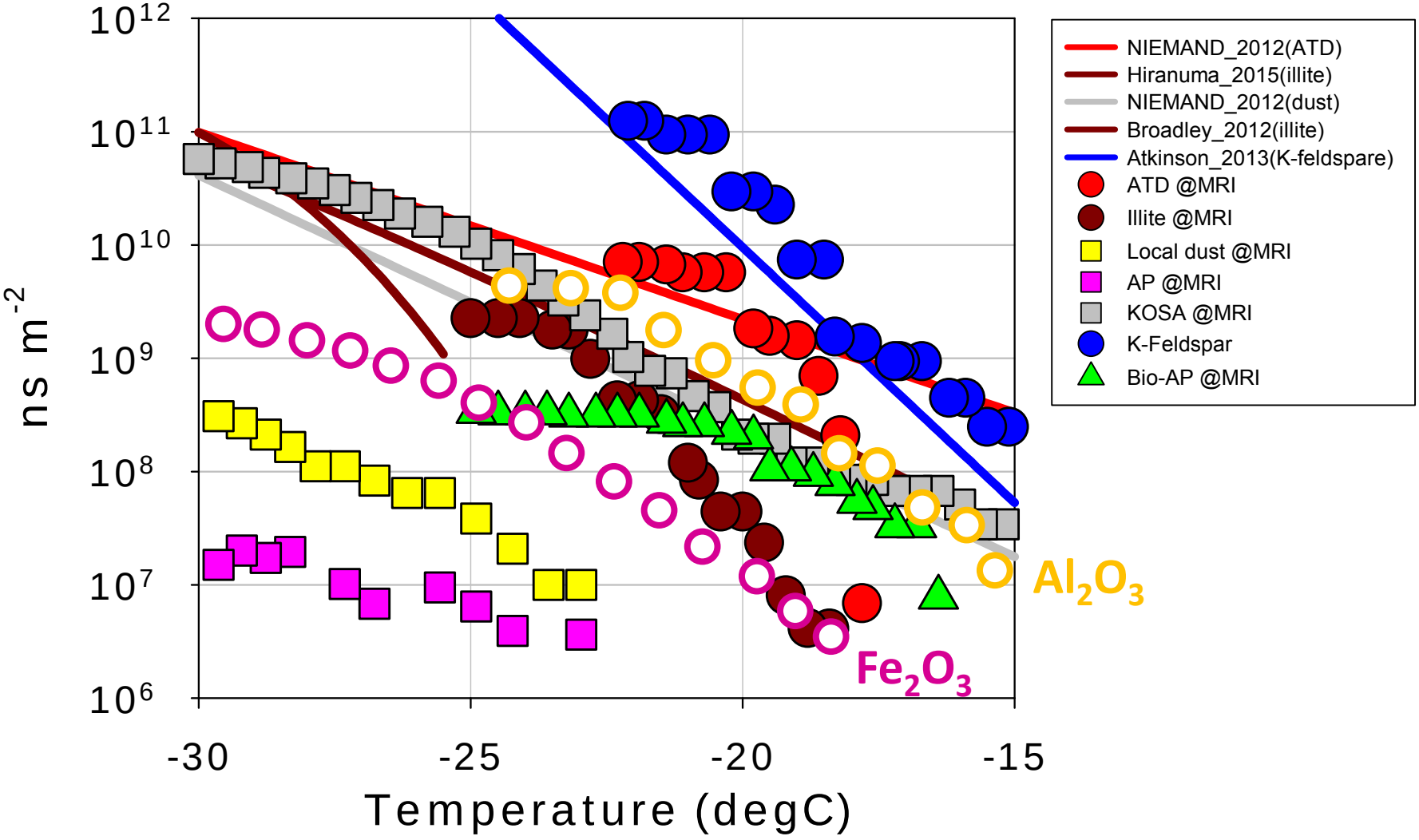
$10^{12}$
$10^{11}$
$10^{10}$
$10^{9}$
$10^{8}$
$10^{7}$
$10^{6}$
ns $m^{-2}$
-30
-25
-20
-15
Temperature (degC)
$Al_2O_3$
$Fe_2O_3$
NIEMAND_2012(ATD)
Hiranuma_2015(illite)
NIEMAND_2012(dust)
Broadley_2012(illite)
Atkinson_2013(K-feldspare)
ATD @MRI
Illite @MRI
Local dust @MRI
AP @MRI
KOSA @MRI
K-Feldspar
Bio-AP @MRI


Thank you for your attention